Embedded-quantum-cluster study of local relaxations and optical properties of Cr^{3+} in MgO

D. J. Groh
Department of Physics, Morningside College, Sioux City, Iowa 51106

Ravindra Pandey
Department of Physics, Michigan Technological University, Houghton, Michigan 49931

J. M. Recio
Departamento de Química Física y Analítica, Universidad de Oviedo, 33006 Oviedo, Spain
(Received 31 May 1994; revised manuscript received 5 August 1994)

Local distortions and optical properties induced by the substitutional Cr^{3+} impurity in the MgO host lattice are computed using the embedded-cluster approach implemented in the ICECAP code. Within this methodology, the impurity centered cluster is described quantum mechanically and is self-consistently coupled with the lattice environment by means of the shell-model treatment of the lattice polarization and distortion. Our calculations predict inward relaxations of the six O^{2-} nearest neighbors surrounding the Cr^{3+} ion for both cubic and noncubic (tetragonal and orthorhombic) configurations in MgO. For the cubic configuration, selected low-lying excited states, including the $10Dq$ generator $^4T_2$, are calculated at several Cr-O separations. After taking into account lattice relaxations and correlation corrections, the computed $10Dq$ value lies 0.19 eV lower than the experimental one. Finally, the response of the Dq parameter and the Cr-O separation to hydrostatic pressure is obtained by performing analogous cluster-in-the-lattice calculations with the lattice parameter of MgO varying according to its equation of state. Analysis of these results reveals that the compressibility at the host cation site is greater than that at the impurity site.

I. INTRODUCTION

Optical transitions within the unfilled $3d^n$ shell of transition metal ions in insulating crystals are of much current interest as examples of tunable four-level laser systems. Chromium doped magnesium oxide ($MgO:Cr^{3+}$) provides such a prototypical system where extensive spectroscopic studies have been performed.[1] It also offers an ideal system to test limitations of theoretical methods investigating local distortions and spectroscopic properties induced by impurities in ionic crystals. This is due to the fact that the impurity Cr^{3+} substituting Mg^{2+} constitutes a charged defect in the lattice that requires a careful treatment of long-range polarization effects in theoretical calculations.

The strength of the distortions experienced by the six O^{2-} ions surrounding Cr^{3+} depends on the local symmetry around the impurity. Besides the most common cubic configuration, tetragonal and orthorhombic arrangements were also reported as produced by nearest cationic vacancies along the [100] and [110] directions, respectively.[2] To the best of our knowledge, direct experimental data of the Cr-O distances have only been reported for the tetragonal configuration, where 1.90 Å and 2.06 Å were obtained after EXAFS (extended x-ray absorption fine structure) and XANES (x-ray absorption near edge structure) experiments on $MgO:Cr^{3+}$.[3] Earlier theoretical and experimental estimations of the Cr-O separation[4–8] (ranging from 1.77 to 2.05 Å) always found the Cr-O distances to be smaller than the experimental Mg-O separation in the pure MgO crystal. This inward relaxation is also the expected conduct from ionic radii arguments.[9] Nevertheless, a unified description of the lattice relaxation considering both defects (the impurity and the vacancy) has not been reported up to date for the three local geometries of Cr^{3+} center in MgO.

Regarding spectroscopic data, there are well-known limitations in the quantum-mechanical methodologies that lead to important discrepancies between the computed and experimental d-d transitions.[8] In the Hartree-Fock approach, the enormous differential correlation effects within the ground and excited states of the cluster prevent a feasible procedure to account for most of the theory-experiment disagreements. However, considering that these differences are appropriately scaled as pressure is applied, computed d-d transitions can offer meaningful information when combined with the corresponding calculated local relaxations. In this way, the relative compressibility at the impurity site with respect to the value at the host cation site can be predicted, and the validity of previous reported data of this magnitude[10] analyzed in a more reliable manner.

In this paper, we seek to examine the accuracy and predictability of an embedded-quantum-cluster method when applied to the investigation of (i) the geometrical positions of the O^{2-} ions in the three arrangements of Cr^{3+} in MgO, (ii) the effects of lattice relaxation and correlation effects on d-d transitions, and (iii) the local

compressibility at the impurity and host cation sites.

The methodology we use here incorporates electronic structure calculations with a classical shell model treatment of lattice polarization and distortion. This method makes a single ansatz, that the perturbation introduced by an impurity in a lattice is confined to a region near that impurity. Beyond that region, its influence can be given in terms of a linear response. This response is manifested by the displacement and polarization of atoms. The region surrounding and including the impurity is called the cluster and is described in the framework of the Hartree-Fock approximation. The response of the remainder of the lattice, called the environment, is treated within the shell model. Applications of this methodology, referred to as ICECAP, have been made to investigate defect and perfect lattice properties in halides and oxides. These applications demonstrated the usefulness of this approach in simulating rather subtle physical features of defects in ionic crystals.[11]

In the following section, we describe briefly the embedded cluster methodology giving the specific details for the calculations performed here. The results are presented and discussed in Sec. III, which is split into three subsections. The first one deals with the three local geometries around Cr^{3+} in MgO, the second one covers the computation of the optical transitions, and the third one contains the study of the pressure effects on the Dq parameter and its relation with the local compressibility.

II. THEORETICAL MODEL

We begin with the description of the molecular cluster consisting of the impurity Cr^{3+} and the six nearest-neighbor O^{2-} ions at the sites (R, 0, 0). The cluster is embedded in a lattice environment of Mg^{2+} and O^{2-} ions located at their crystallographic positions in the pure MgO rocksalt structure [R(Mg-O)=2.106 Å]. In this way, we assume that Cr^{3+} significantly disrupts the atomic ordering and electronic distribution of MgO only in a small region described by the nearest-neighbor O^{2-} ions. The cluster ions will be described within the framework of the unrestricted Hartree-Fock approximation. The rest of the MgO lattice, where the perturbation due to Cr^{3+} is assumed to be weak, will be simulated by the classical shell model.

In the shell model, an ionic lattice is described in terms of point charges interacting by pairwise potentials. Ionic polarization effects are included by associating two charges with each ion, a shell and a core charge, Y and (Q-Y), respectively, where Q is the total ionic charge. The shell and the core of a given ion are assumed to be coupled by a harmonic potential so that the displacement of the shell relative to the core describes the polarization. All the point charges in the lattice interact through Coulomb potentials, except for the core and the shell of the same ion. In addition, short-range potentials act between shells of ions that are nearest neighbors. Various forms of short-range potentials have been previously employed. For the present work, we use the Buckingham potential of the form

$$V(X) = Be^{-\frac{X}{\rho}} - \frac{C}{X^6} , \tag{1}$$

where X is the shell-shell separation, and B, ρ, and C are parameters that are generally fitted, simultaneously with Q and Y, to bulk properties, such as cohesive energy, lattice spacing, elastic and dielectric constants and phonon spectra. In the present work, these parameters for MgO are taken from Sangster and Stoneham.[12] Successful applications of the shell model include not only nonelectronic point defects but dislocations and interfaces of ionic and semi-ionic materials. For details, we refer to a review edited by Catlow and Mackrodt.[13]

The electronic structure of the quantum-mechanical molecular cluster containing the impurity and nearest-neighbor ions can be obtained by solving the Fock equations in the unrestricted Hartree-Fock self-consistent-field (UHF-SCF) approximation. The procedure followed is based on the technique described by Roothaan,[14] where the molecular orbitals are linear combinations of atomiclike basis orbitals constructed from Gaussian primitive functions. For Cr^{3+}, we begin with the (533/53/5) basis set given by Huzinaga[15] and then use a total energy optimization procedure to add s, p, and d type diffuse Gaussian primitives, which are expected to describe more accurately the excited states. The resulting basis set for Cr^{3+} consists of $4s$, $3p$, and $2d$ orbitals with a (5331/532/52) contraction.[16] For the nearest-neighbor O^{2-} ions, we have used the (77/4) basis set[17] whose p-type primitives are split along the Cr-O axis for greater variational freedom to the wave function.

Total energy of a crystalline lattice with an embedded quantum cluster can be written as

$$E = E_C + W_Z + W_E , \tag{2}$$

where E_C is the Hartree-Fock total energy for the cluster, including Coulombic interaction with the embedding lattice, W_Z is the Coulomb energy of the cluster nuclei interacting among themselves, and W_E is the interaction energy of the embedding lattice ions (shells and cores) among themselves plus their short-range interaction with the cluster. Total energy, E, is now minimized with respect to all shell and core positions of the embedding lattice (i.e., lattice configuration) and simultaneously with respect to variational parameters of the cluster wave function (i.e., electronic configuration). This minimization is updated while the nuclear positions of the cluster ions (i.e., cluster configuration) are varied to yield overall minimization of the total energy.

Note that the quantum-mechanical molecular cluster is embedded in the classical shell-model lattice. As a consequence, the cluster is seen by its environment as a Coulomb potential, and also by means of short-range interactions of the cluster ions with point-charge ions. The electrostatic potential of the cluster, expressed as a multipole electric moment series, can be calculated from its nuclear positions and electronic wave function, and simulated by a small number of point charges. Since these moments must be consistent with the polarization that they produce in the embedding lattice, the calculations for the cluster Hartree-Fock solution and lattice polar-

ization are iterated until convergence for a given cluster configuration. This multipole consistency step turns out to be a very fast-converging process, and is repeated for each step in the variation of the cluster configuration.

III. RESULTS AND DISCUSSION

A. Local relaxations

As we have pointed out above, experimental studies have shown that the impurity Cr^{3+} substituting Mg^{2+} in MgO can have a geometrical arrangement with either cubic or noncubic symmetry.[18,19] A noncubic symmetry arises when the charge-compensating Mg^{2+} vacancy occupies a near-neighbor position along either a [100]-type direction (tetragonal site, C_{4v} symmetry) or a [110]-type direction (orthorhombic site, C_{2v} symmetry). If we restrict the exploration of the local distortions to the Cr^{3+} nearest neighbors, we have the six O^{2-} ions at the same R'(Cr-O) distance in the O_h cluster, but three different R'(Cr-O) values in the C_{4v} and C_{2v} clusters. Also, it becomes necessary to specify the values of one and three of the O-Cr-O bond angles to completely determine the geometry of the C_{4v} and the C_{2v} arrangements, respectively. On the other hand, we have observed that the displacements suffered by the ions beyond the nearest-neighbor positions of the defect, with respect to the host lattice geometry, are progressively smaller, the anion being always more affected than the cation. In any case, beyond the region considered in the calculations ($\sim$ 5 Å around the defect), the ionic displacements do not alter the final solution of the total energy minimization procedure.

To calculate the above set of structural parameters, we have organized our computations in two steps. First, we carry out the optimization of the R'(Cr-O) variable in the ground state ($^4A_2$) of the cubic configuration (O_h) at the unrestricted Hartree-Fock (UHF) and the UHF plus correlation corrections through second order many-body perturbation theory[20] (UHF+MBPT) levels. At both the levels (UHF and UHF+MBPT), the calculated equilibrium configurations are nearly the same: the nearest-neighbor O^{2-} ions relaxes inward by 3.6%, with R'(Cr-O)=2.03 Å. When we reduce the size of the quantum cluster to a single Cr^{3+} ion, the O^{2-} ion relaxes towards the Cr^{3+} by 4%. In spite of the limited SCF active space, the equilibrium configuration shows an excellent agreement with the more expensive UHF and UHF+MBPT calculations on the octahedral (seven-ion) cluster. Within the single-ion-in-the-lattice strategy, we can therefore investigate in a systematic and equivalent manner the effects of the impurity and vacancy on the local environment in a computationally efficient way. Such effects are qualitatively illustrated in Figs. 1(a)–1(d) and quantitatively given in Table I. In this table we also include the configurational parameters obtained from the ionic radii data of Shannon,[9] data from EXAFS and XANES experiments,[3] and the predictions obtained after shell-model computations,[4] application of the lattice relaxation model,[7] *ab initio* cluster-in-the-lattice calculations,[8] and fittings to spectroscopic data.[5,6]

The most interesting conclusions emerging from the analysis of our computations can be summarized in the following four points: (i) Nearest-neighbor ions are attracted by the Cr^{3+} impurity and are repelled by the cation vacancy, the repulsion being greater than the attraction. This behavior is fully consistent with the fact that the Cr^{3+} impurity and the vacancy have net charges of +1 and −2 in the lattice, respectively. (ii) The simultaneous effect of the two point defects is lower than the sum of their individual effects. Besides, the repulsion induced by the vacancy shows a rapid decay with the distance. (iii) Our computations are in good agreement with the ionic radii expectations[9] for the R'(Cr-O) value in the O_h symmetry and with the experimental data reported for the C_{4v} configuration.[3] (iv) The calculated distortions for the three configurations are consistent with each other and lead to a very satisfactory global picture of the local geometry of Cr^{3+} centers in MgO.

The above conclusions support our predictions when compared with the rest of R'(Cr-O) and bond angle estimations. It is interesting to note that for the octahedral configuration we obtain a value only 0.01 Å smaller than the one reported when the CrO_6^{9-} cluster is embedded in a quantum lattice,[8] which coincides with our prediction from the seven-ion cluster. The extrapolation of Sangster,[4] based on the local distortions induced by a series of trivalent $3d$ ions in MgO, seems to overestimate the strength of the impurity effect, leading to a too short Cr-O separation. The same can be said after the analysis of the data reported by Yeung (who has strongly criticized the approach of Du and Zhao[5]) for the C_{4v} configuration.[7] In this case, we observe that the clear effect of the vacancy, manifested in the large O_1-Cr-O_4 angle and the short Cr-O_1 distance, is balanced by the strong attraction of the impurity center which produces a Cr-O_3 separation similar to our prediction. Finally, the only previous estimation of the local geometry for the orthorhombic configuration[6] is in good agreement with the calculation presented here.

B. Optical transitions

Potential energy surfaces of the t_2^3-$^4A_2$ ground state and the t_2^3-^2E and $t_2^2e^1$-$^4T_2$ excited states of Cr^{3+} doped MgO have been obtained at the UHF+MBPT level in the cubic configuration (see Fig. 2). Note that the quantum cluster is embedded in the shell-model lattice. The calculated results allow us to evaluate the $10Dq$ parameter, (i.e., the energy involved in the t_2^3-$^4A_2 \rightarrow t_2^2e^1$-$^4T_2$ absorption), the R-line phosphorescence (t_2^3-$^2E \rightarrow t_2^3$-$^4A_2$ transition), and the $t_2^2e^1$-$^4T_2 \rightarrow t_2^3$-$^4A_2$ broad fluorescence band. Although these magnitudes belong to some of the more interesting features of the optical spectrum of Cr^{3+} doped MgO (see Ref. 21 and references therein), we will not attempt to provide a detailed comparison with experimental data or other calculated values. Our aim is restricted to give an illustration of the ICECAP ability in the study of the electronic transitions located at the Cr^{3+}

site. In particular, we are interested in the analysis of the geometrical relaxations and the correlation effects on the low-energy transitions.

The computation of the three transitions specified above is carried out using the so-called ΔSCF method, i.e., taking the difference in energy between the two electronic states involved in the transition. We began with the calculation of the transition energies in the frozen-lattice configuration, where the Cr-O separation is taken to be the experimental R(Mg-O) value in the host lattice. Here, absorption and fluorescence, obviously, lie at the same energy (1.51 eV at the UHF+MBPT level). When the lattice relaxation is taken into account, absorption and fluorescence lie 0.30 eV and 0.22 eV, respectively, above the corresponding values at the frozen lattice. For the R-line (phosphorescence) transition, the effect of the lattice relaxation is, however, almost negligible: 1.62 eV and 1.63 eV when the lattice is frozen and relaxed, respectively (see Fig. 2).

The indirect lattice effect induced by means of the equilibrium distance in the computed spectroscopic frequencies can be meaningfully related with the character of the transition.[8] For the intraconfigurational t_2^3-$^2E \rightarrow t_2^3$-$^4A_2$ transition (which is $10Dq$ independent), it is not expected that the lattice affects in a different manner the two states involved, as this is a transition well localized in the metal. An illustration of this fact is that the equilibrium configuration is calculated to be the same (2.03 Å) for both states. For the interconfigurational transitions involving the t_2^3 and $t_2^2e^1$ configurations (which are $10Dq$ dependent), we expect a lowering of the transition frequency as the R'(Cr-O) value increases. It is worthwhile to note that the computed absorption energies at the frozen-lattice (1.51 eV) and relaxed-lattice (1.81 eV)

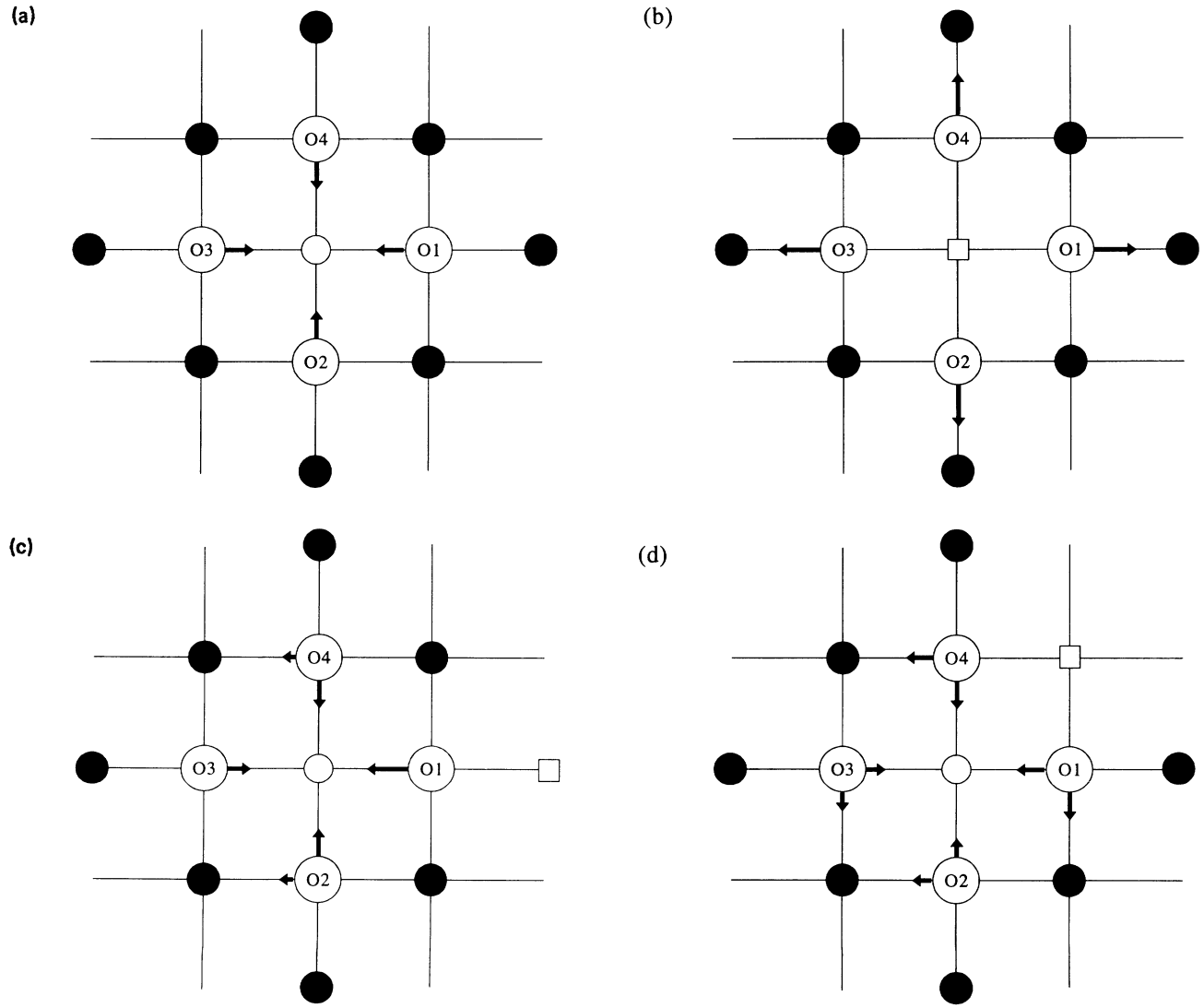

FIG. 1. Qualitative diagrams of the O^{2-} distortions induced by (a) a Cr^{3+} impurity, (b) a Mg^{2+} vacancy, (c) a combined Cr^{3+}-[100]Mg^{2+} vacancy, and (d) a combined Cr^{3+}-[110]Mg^{2+} vacancy in the MgO host lattice. Only the movement of the four O^{2-} ions (O1-O4) in the x-y plane is shown. Black filled circles represent Mg^{2+} ions, the empty circle and the empty square represent the Cr^{3+} ion and the vacancy, respectively.

TABLE I. Local geometry of the six O^{2-} ions surrounding Cr^{3+} in the three configurations reported for the MgO:Cr^{3+} system. See Fig. 1 for notation. Numbers in brackets are reported uncertainties in the last digit. Distances are in Å, bond angles are in degrees.

	Present	Other data
O_h		
R'(Cr-O)	2.02	2.02,[a] 1.85,[b] 2.03[c]
C_{4v}		
R'(Cr-O_1)	1.92	2.050(4),[d] 1.7720,[e] 1.90(3)[f]
R'(Cr-O_2)	2.03	1.9438,[e] 2.06(4)[f]
R'(Cr-O_3)	2.04	2.0277[e]
O_1-Cr-O_4	90.7	94.02[e]
C_{2v}		
R'(Cr-O_1)	1.99	1.94[g]
R'(Cr-O_2)	2.06	
R'(Cr-O_5)	2.04	
O_1-Cr-O_4	99.2	98.2[g]
O_2-Cr-O_3	87.6	
O_5-Cr-O_6	166.8	

[a]Crystal radii, Ref. 9.
[b]Shell model, Ref. 4.
[c]*Ab initio* cluster-in-the-lattice calculations, Ref. 8.
[d]Fitting to spectroscopic data, Ref. 5.
[e]Application of the lattice relaxation model, Ref. 7.
[f]Extended x-ray absorption fine structure and XANES, Ref. 3.
[g]Fitting to spectroscopic data, Ref. 6.

levels follow the expected distance sequence: 2.106 Å and 2.03 Å, respectively. Moreover, at the equilibrium configuration found for the $^4T_2$ state [R'(Cr-O)=2.05 Å], the fluorescence lies between the two previous values (1.73 eV), confirming the correlation between interconfigurational transitions and Cr-O separations.

We now proceed to discuss electron correlation effects on the computation of electronic spectroscopic frequencies. Note that the inclusion of the correlation corrections (MBPT) does not modify significantly the UHF equilibrium configurations. However, after the correlation corrections are taken into account, there is an overall better agreement between the computed and observed transition data. As an example, the UHF, UHF+MBPT, and experimental values for the absorption energies show the following progression: 1.74 eV, 1.81 eV, and 2.00 eV. It is to be noted that the correlation corrections increases (decreases) the values obtained for the absorption (phosphorescence), as corresponds to the expected opposite shifts suffered by the $^4T_2$ and ^2E curves with respect to the ground state in the UHF+MBPT calculations. In general, the discrepancies obtained with respect to the observed data[1,22] are less than 10% in the case of our more refined calculation (UHF+MBPT and fully relaxed lattice). When the magnitudes involve differences between two transitions, as in the $^4T_2 \rightarrow {}^2E$ nonradiative transition or in the vertical Stokes shift (Δ_s), the agreement is greatly improved (see Table II) which should be seen as an indication of the consistency of our computational method. Nevertheless, these calculated energies are to be taken with caution because the computed differences do not involve vibrational effects, and they may play an important role for such small quantities. Besides, the spin-orbit coupling of the two excited states will alter not only the energy differences but also the spin identity of the states.

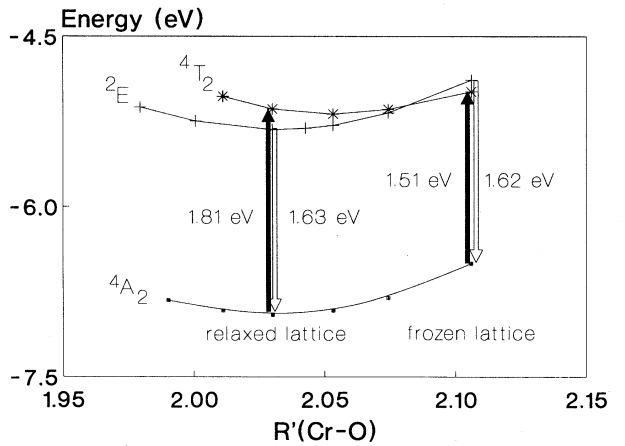

FIG. 2. Potential energy surfaces for the ground state and low-lying excited states of MgO:Cr^{3+} at the UHF+MBPT calculations in the cubic configuration. Symbols represent calculated values. The absorption (filled arrow) and phosphorescence (empty arrow) transitions are illustrated for the relaxed- and frozen-lattice configurations. Units for R'(Cr-O) are Å.

C. Pressure dependence of Dq and local compressibility

In spite of the different definition of the $10Dq$ parameter in the crystal-field theory and in the HF-SCF molecular orbital approach,[23] it is generally assumed that the computed absorption energy changes approximately with R'(Cr-O) according to this equation:

$$10Dq = CR'^{-5} , \tag{3}$$

which is only exact in the point-charge crystal-field framework.[24]

To verify the above suggestion, we investigate the pressure dependence of the Dq parameter up to 30 GPa. At each given hydrostatic pressure (0, 2.15, 4.95, 8.23, 16.87, and 29.9 GPa), we obtain the corresponding R(MgO) values (2.106, 2.097, 2.086, 2.074, 2.046, and 2.011 Å) using the experimental equation of state.[25] We then perform total energy computations at the UHF+MBPT level in the $^4A_2$ ground state to determine the equilibrium R'(Cr-O) configurations at each lattice parameter value. At the computed optima R' separations [R'(Cr-O)=2.030, 2.026, 2.021, 2.016, 2.001, and 1.9849 Å], we use the vertical approximation to calculate the energy of the $^4T_2$ state and then generate $10Dq$ values by total energy differences. If Eq. (3) is valid to describe the $10Dq$ variation with R'(Cr-O), the $\log_{10}\frac{Dq(R')}{Dq_0}$ versus $\log_{10}\frac{R'_0}{R'}$ plot should be a straight line with slope equal to 5. In these expressions the subscript 0 means zero pressure.

Such a log-log plot appears in Fig. 3 with a slope of 4.8 demonstrating that Eq. (3) describes accurately the $Dq(R')$ function in the present case. Moreover, Fig. 3

TABLE II. Computed relaxed lattice and observed data for the transitions involving the ground state and low-lying excited states of cubic Cr^{3+} doped MgO. Δ_s stands for the vertical Stokes shift. Values in eV.

	$^4A_2 \rightarrow {}^4T_2$	$^2E \rightarrow {}^4A_2$	$^4T_2 \rightarrow {}^4A_2$	$^4T_2 \rightarrow {}^2E$	Δ_s
UHF	1.74	1.74	1.70	-0.07	0.04
UHF+MBPT	1.81	1.63	1.73	0.10	0.08
Experimental	2.00[a]	1.78[a]	1.91[b]	0.13[b]	0.09

[a]Reference 1.
[b]Reference 22.

also shows an increase of 11% in Dq at 30 GPa with respect to its zero pressure value. Similarly, experimental studies on ruby have found that Dq increases by 15% at 30 GPa.[26] However, when our values are compared with the data reported by Minomura and Drickamer[10] on Cr^{3+} doped MgO, there is an apparent disagreement since 11% increase is already obtained in their experiments at 10 GPa. We do not have any plausible explanation for these contradictory results. Nevertheless, it is to be noted that the Dq-pressure curve obtained by Minomura and Drickamer shows an asymptotic behavior after approximately 10 GPa. In analogous experiments on ruby,[27] Stephens and Drickamer observed again the same conduct, which contrasts with the trend (almost linear) of the corresponding function in the more recent experiments of Duclos *et al.*[26]

A similar log-log plot involving Dq and the R(Mg-O) separation, instead of R'(Cr-O), is included in Fig. 3. It is easy to demonstrate[28] that when the slope of the straight line obtained for $X = R$(Mg-O) is less than the one for $X = R'$(Cr-O), the local compressibility at the host cation site is greater than that at the impurity site. Such result can be directly inferred from the R(Mg-O) and R'(Cr-O) values reported above: the Mg-O and Cr-O separations in MgO are reduced by 4.5% and 2.2%, respectively, when pressure changes from 0 to 30 GPa. This behavior seems to be reasonable, since it is expected that the Cr^{3+}-O^{2-} bond will be stronger than the Mg^{2+}-O^{2-} one because of the extra positive charge. Support to our predicted conduct is also found from other arguments. Accordingly, Sangster[4] has studied the effects of hydrostatic and uniaxial stress on impurity-doped ionic crystals concluding that the strain around the impurity is proportionality to the strain induced in the host lattice. The proportional constant is about one for isovalent impurities, but lower than one for impurities introducing extra positive charges in the lattice. Zheng[29] has also remarked that the discrepancies between calculated and experimental spin-lattice coupling coefficients for MgO:Cr^{3+} can be resolved if the crystal were harder in the vicinity of the impurity, which would lead to reductions of local strains.

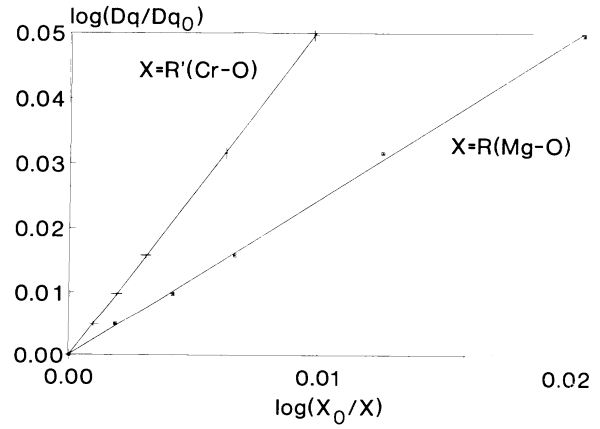

FIG. 3. Log_{10}-log_{10} plot of the reduced crystal-field splitting parameter (Dq/Dq_0) versus the inverse of reduced distances (X_0/X).

Contrary to the above picture, the analysis of Minomura and Drickamer's experimental data reveals that the compressibility at the Cr^{3+} site is greater by a 1.12 factor than that at the host cation site. This conclusion emerges from the log-log plot they obtained using Bridgman's data for the MgO equation of state[30] and employing Eq. (3) for the Dq dependence on R'(Cr-O). Since in this case the theory-experiment mismatch involves not only our data, but the conclusions from the analysis of other different phenomena, it is relevant to suspect that some of the assumptions taken to infer the local compressibility from the experiments are not appropriate. For example, the use of the pure MgO equation of state to describe the pressure values of the Cr^{3+} doped MgO system is only exact in the limit of infinite dilution. This ideal condition is given in our computer simulations but not in the real experiments. In that way, a finite concentration of the Cr^{3+} impurity (not reported in Minomura and Drickamer paper) may modify the true lattice parameter at a given pressure with respect to the predicted value using the MgO equation of state. It is expected, finally, that those changes increase with the impurity concentration and as the pressure is applied. Therefore, we believe that further experimental investigation on the response of the local properties (such as d-d transitions) to pressure for the MgO:Cr^{3+} system is warranted in order to clarify the discrepancies reported in this work.

ACKNOWLEDGMENTS

We thank Professor M. Flórez and Professor E. Francisco for helpful discussions and the careful reading of the manuscript. One of us (J.M.R.) thanks the Spanish Ministerio de Educación y Ciencia and the Fulbright Commission for a grant that has made possible his stay at Michigan Technological University. Partial financial support from NATO collaborative Grant No. CRG921348 and the computational facilities from ASCC center at MTU are also acknowledged.

[1] M. B. O'Neill and B. Henderson, J. Lumin. **39**, 161 (1988).
[2] B. Henderson and J. E. Wertz, *Defects in the Alkaline Earth Oxides* (Taylor & Francis, London, 1977).
[3] K. Asakura and Y. Iwasawa, Mater. Chem. Phys. **18**, 499 (1988).
[4] M. J. L. Sangster, J. Phys. C **14**, 2889 (1981).
[5] M. L. Du and M. G. Zhao, J. Phys. C **19**, 2935 (1986).
[6] X. P. He and M. L. Du, Phys. Status Solidi 144, K51 (1987).
[7] Y. Y. Yeung, J. Phys. Condens. Matter **2**, 2461 (1990).
[8] L. Pueyo, V. Luaña, M. Flórez, E. Francisco, J. M. Recio, and M. Bermejo, Rev. Solid State Sci. **5**, 197 (1991).
[9] R. Shannon, Acta Crystallogr. Sec. A **32**, 751 (1976).
[10] S. Minomura and H. G. Drickamer, J. Chem. Phys. 35, 903 (1961).
[11] J. Vail, R. Pandey, and A. B. Kunz, Rev. Solid State Sci. **5**, 241 (1991).
[12] M. J. Sangster and A. M. Stoneham, Philos. Mag. B **43**, 597 (1981).
[13] *Computer Simulation of Solids*, edited by C. R. A. Catlow and W. Mackrodt (Springer-Verlag, Berlin, 1982).
[14] C. C. J. Roothaan, Rev. Mod. Phys. **32**, 179 (1960).
[15] S. Huzinaga, *Gaussian Basis Sets for Molecular Calculations* (Elsevier, New York, 1984).
[16] The exponents and contraction coefficients of the basis set can be obtained from the authors.
[17] R. Pandey and J. M. Vail, J. Phys. Condens. Matter **1**, 2801 (1989).
[18] J. E. Wertz and P. V. Auzins, Phys. Rev. **106**, 484 (1957).
[19] C. M. McDonagh, B. Henderson, G. F. Imbusch, and P. Dawson, J. Phys. C **13**, 3309 (1980).
[20] See, for example, D. J. Thouless, *The Quantum Mechanics of Many-Body Systems*, 2nd ed. (Academic Press, New York, 1972), Chap. 4.
[21] K. Dunphy and W. W. Duley, J. Phys. Chem. Solids **51**, 1077 (1990).
[22] M. O. Henry, J. P. Larkin, and G. F. Imbusch, Phys. Rev. B **13**, 1893 (1976).
[23] M. Bermejo and L. Pueyo, J. Chem. Phys. **78**, 854 (1983).
[24] S. Sugano, Y. Tanabe, and H. Kamimura, *Multiplets of Transitional-Metal Ions in Crystals* (Academic, New York, 1970).
[25] I. Jackson and H. Niesler, in *High-Pressure Research in Geophysics*, edited by S. Akimoto and M. H. Manghnani (Academic, Tokyo, 1982), p. 93.
[26] S. J. Duclos, Y. K. Vohra, and A. L Ruoff, Phys. Rev. B. **41**, 5372 (1990).
[27] D. R. Stephens and H. G. Drickamer, J. Chem. Phys. **35**, 427 (1961).
[28] J. M. Recio, E. Francisco, and M. Flórez (unpublished).
[29] W. C. Zheng, J. Phys. Condens. Matter **1**, 8093 (1989).
[30] P. W. Bridgman, Proc. Am. Acad. Arts Sci. **77**, 220 (1949).